JOURNAL OF SPACECRAFT AND ROCKETS
Vol. 29, No. 2, March-April 1992

Launch Dynamics of Fin-Stabilized Projectiles

J. Bornstein,* I. Celmins,† P. Plostins,* and E. Schmidt‡
U.S. Army Ballistic Research Laboratory, Aberdeen Proving Ground, Maryland 21005

An experimental methodology examining the disturbances acting upon fin-stabilized projectiles during the launch process and initial stages of free flight has been developed. Disturbances are characterized by the angular deviation of the projectile trajectory from an anticipated line of flight extending between the gun muzzle and the aim point prior to firing the cannon. Gun motion during projectile in-bore time is determined using strain gauges and proximity probes. A technique employing multiple orthogonal x rays is used to measure both the linear and angular motion of the projectile during the transitional ballistic flight phase. Radiographs taken in the immediate vicinity of the muzzle provide the relative motion of the projectile with respect to the muzzle caused by in-bore balloting, gun/projectile decoupling, initial sabot discard, and muzzle blast disturbances. Comparison with radiographs obtained after sabot separation measures the disturbances due to asymmetric sabot discard. Results obtained using these techniques have shown that the gun dynamics contributes less than half of the overall disturbance to the projectile, but the in-bore vibration of the projectile is a major contributor, as is asymmetric sabot discard.

Nomenclature

C_L = lift coefficient
C_M = pitching moment coefficient
ξ = yaw angle of projectile
ξ' = yaw rate of projectile

Subscripts

o = initial value
α = derivative with respect to angle of attack

I. Introduction

TWO requirements have driven the development of improved fin-stabilized ammunition for tank main guns: improved penetration and increased accuracy. Improved penetration may be accomplished through the design of warheads for chemical energy ammunition or the employment of heavier penetrator rods traveling at higher velocities for kinetic energy ammunition. Improved accuracy requires minimizing the magnitude or variability of the disturbances acting on a projectile during launch and free flight.

No single quantity fully describes the accuracy of ammunition; rather, a hierarchy of values is used. These include the ammunition dispersion or the standard deviation of a series of impacts obtained from a single gun firing one type and lot of ammunition during a single occasion, the group center of impact, and center of impact variations between gun tubes and between tanks. The term jump refers to the deviation of the group center of impact from the aim point.

Ammunition accuracy is affected by many disturbances. Prior to launch, the gun is aimed at a target, the propellant charge is ignited, and the high-pressure combustion gases propel the round forward in the gun tube. These gases exert a force upon the breech, causing it to recoil rearward in its mount. If the center of pressure is laterally offset from the gun system center of mass, a moment is produced which causes the gun tube to rotate around the trunnions. Although an idealized cannon bore is perfectly straight, gun tubes typically possess curvature due to machining, droop under gravity, and firing dynamics. Interactions between the gun tube and projectile also occur, causing a mutual exchange of transverse momentum. Thus, the muzzle no longer points where it was initially aimed at the instant the projectile is launched.[1]

A modern saboted kinetic energy round consists of a subcaliber fin-stabilized penetrator rod encased within a lightweight, elastic sabot. The combination may be considered as a system of spring/mass elements, subjected to side forces as it follows the irregular curvature of the gun. The resulting transverse motion causes the projectile/sabot to ballot and vibrate giving it a linear velocity which is not aligned with the gun tube centerline and an angular velocity about its own center of gravity (c.g.). Within the gun tube, the combination is supported at two points along its length. As it exits the gun, it sequentially loses the support of these two boreriders. During decoupling, conditions can arise which result in a force and/or moment being imparted to the projectile/sabot.

During the initial few meters of flight, the projectile flies through the muzzle blast. The projectile is subjected to abnormal ambient conditions, resulting from the outward flow of gas from the gun muzzle over the rear of the projectile. The resulting pressure distribution on the projectile can give rise to forces and moments that deflect it from its initial trajectory.

The process of sabot separation begins as the bullet leaves the gun tube. Because of the transverse motion of the projectile within the gun, energy is stored in the elastic sabot petals. As the projectile leaves the muzzle, the constraints of the gun tube are released and the sabot elements are able to move laterally outward. Aerodynamic forces acting on each of the sabot petals causes them to lift up and disengage from the buttress grooves of the penetrator rod. Despite the higher drag forces acting on each petal, the sabot elements will fly in close proximity to the penetrator for several meters downrange. Aerodynamic interaction between the sabot and projectile will occur throughout this period. Asymmetric shock waves, formed due to the supersonic flight of the sabot elements, impinge upon the penetrator body and fins, imparting disturbances. Ultimately the sabot petals move sufficiently far from the penetrator, either to the side or rear, to prevent further interaction and the penetrator is in free flight. However, in the process, both aerodynamic and mechanical disengagement asymmetries can result in a significant net force and moment being applied to the penetrator.[2]

Presented as Paper 89-3395 at the AIAA Atmospheric Flight Mechanics Conference, Boston, MA, Aug. 14-16, 1989; received May 18, 1990; revision received May 17, 1991; accepted for publication June 21, 1991.

*Aerospace Engineer, Launch and Flight Division. Member AIAA.
†Aerospace Engineer, Launch and Flight Division.
‡Chief, Fluid Physics Branch, Launch and Flight Division. Associate Fellow AIAA.

As the projectile enters free flight, it has an initial yaw angle ξ_0 and rate ξ_0'. This results in a deflection of the trajectory known as aerodynamic jump. For most finned projectiles of interest, the initial rolling motion is negligible and the magnitude of this term can be determined from the values of C_{M_α}, C_{L_α}, and ξ_0', as shown by Murphy.[3]

Lastly, the projectile is subject to both crosswinds and gravity as it flies downrange. The effect of gravity is primarily dependent upon the time of flight to the target and can be determined from a knowledge of the projectile drag coefficient, initial velocity, and range to the target. The influence of crosswinds will be a function of the projectile geometry and the range to the target. For the tests discussed in this paper, the initial portion of the projectile trajectory was indoors, through the Ballistic Research Laboratory (BRL) Transonic Range Facility, thus minimizing the impact of crosswinds upon the results.

Each disturbance source can potentially affect accuracy, either jump or dispersion. To approach the problem of maximizing accuracy rationally, it is necessary to quantify the contribution of each disturbance. An initial study of this problem was conducted by Gay and Elder.[1] In a combined theoretical and experimental analysis of a 90-mm gun system, they examined both gun dynamics and projectile free-flight yawing motion, noting that these sources alone could not account for the observed jump. They concluded that other sources such as projectile in-bore motion must make major contributions. A more recent paper by Biele,[4] which confined itself to measurements of gun vibration and projectile free-flight motion, suggested that asymmetries in the sabot discard process also might account for significant contributions to jump.

A methodology to examine the complete launch dynamics problem has been developed at BRL and has been utilized to examine the behavior of ammunition for the 105-mm and 120-mm main guns of the M1 and M1A1 tanks. This paper will provide an overview of the test methodology and instrumentation required to measure the launch disturbances and the "closure analysis" which unifies the jump components, indicating the contribution of each disturbance to the overall projectile jump.

II. Methodology

To quantify the effects of various disturbance sources, the overall jump of the projectile has been divided into component parts which can be physically measured. Figure 1 depicts the closure analysis for a typical saboted round. Each disturbance is represented by a vector equal to the deviation of the projectile trajectory, in angular coordinates, caused by the disturbance. In some instances, multiple sources act at a given point in the projectile trajectory and separation of the contributions is not possible. Under these circumstances, it is necessary to lump the deviation due to a number of disturbances into a single vector.

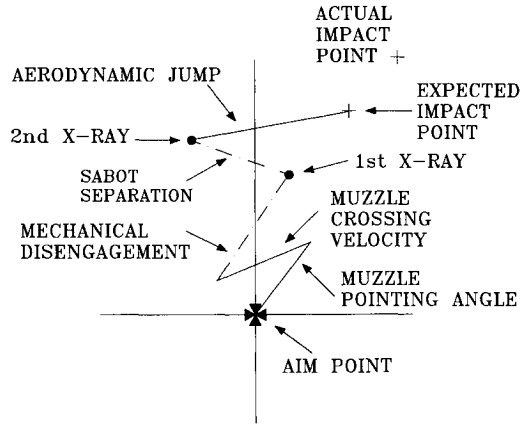

Fig. 1. Vector diagram indicating the closure analysis with sources of disturbance to the projectile trajectory.

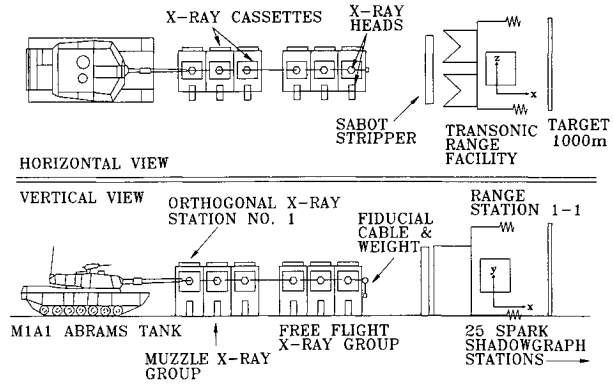

Fig. 2 Schematic diagram of setup for tests.

If all of the disturbances have been accurately measured, the vector sum of the individual components will be identical to the actual target impact point, yielding closure. From an analysis of the error sources associated with each of the measurement techniques, it has been concluded that under optimal circumstances the analysis is accurate to approximately 0.2 mrad. Thus, cases for which the difference between the summation of the measured disturbances and the actual impact point is less than 0.2 mrad will be said to exhibit closure.

Figure 2 is a sketch of the experimental setup for the tests. All tests were conducted from a tank-mounted cannon firing at a target located approximately 1 km distant. The cannon is aimed directly at the target cross using a collimated muzzle bore telescope and no superelevation is used to compensate for gravity. On the gun and between the muzzle and the target, a wide variety of instrumentation has been utilized to determine both the gun dynamics and the motion of the projectile as it flies downrange.

The gun dynamics contribution to the overall jump, measured using a combination of proximity probes and strain gauges, is represented by two vectors in Fig. 1. The first begins at the aim point, denoted by the central cross in the figure, and represents the muzzle pointing angle at the instant of projectile launch. The second vector indicates the deflection due to the velocity of the gun tube perpendicular to the line of flight (i.e., ratio of transverse muzzle velocity and projectile forward velocity).

Because of obscuration by the propellant gases and muzzle flash, it is not possible to directly photograph the projectile as it is launched. X-ray radiography is therefore utilized to determine the initial trajectory of the projectile. Six orthogonal x-ray stations are located just downrange of the muzzle. The first three stations are placed close to the muzzle and observe the projectile just after it exits the gun and during the initial stages of the sabot discard process. The photographic data obtained from these x rays provides both the initial yawing rates and linear c.g. motion of the projectile as it is launched. The deviation of the linear c.g. motion of the projectile from the preshot line of fire is represented on the closure diagram by the point which is marked "1st x ray." The dashed line between the end of the gun dynamics vector and this point represents the sum of the disturbances caused by in-bore balloting motion, projectile "tip-off," muzzle blast, and the initial stages of the sabot disengagement from the subprojectile. This series of disturbances will be referred to as the mechanical disengagement phase.

The second three orthogonal x-ray stations are located further downrange, after the sabot has completely separated and the projectile has entered free flight. The projectile trajectory determined from these x rays is shown in the diagram by the point which is marked "2nd x-ray." The disturbance represented by the difference in the projectile trajectory measured by the two groups of x rays is due to asymmetric sabot discard. The final vector in the diagram is the aerodynamic jump of the projectile.

After launch, the projectile flies through the BRL Transonic Range where it is photographed at 25 orthogonal spark shadowgraph stations covering 208 m of the trajectory. The position and attitude of the projectile is defined from this data and forms the basis for the determination of both aerodynamic and trajectory characteristics. The trajectory provides a redundant measurement of properties near the gun and at the target. By extrapolating back toward the weapon, the Transonic Range data fit provides a verification of the x-ray data. Extrapolation downrange provides a check on the target impact information.

In the following sections, each of the measurement techniques used in the analysis will be briefly discussed. Data obtained for the flight of a saboted cone stabilized training projectile (TPCSDS-T) will be used to illustrate both the measurement techniques and the closure analysis.

III. Gun Dynamics

Although the in-bore time for a projectile is relatively short, the forces and moments exerted upon the gun tube by the high pressure combustion gases and the projectile are sufficient to cause a significant transverse motion of the tube prior to shot exit. This motion is due to the rotation of the gun about its support bearing and the elastic vibration of the tube reacting to both the high-pressure propellant gases and interaction with the projectile.

In previous gun dynamics investigations, a variety of experimental techniques have been utilized, including optical methods,[3] inductive transducers,[5] and strain gauges.[6] The current method is a refinement of the technique utilized by Biele,[4] treating the gun tube as an elastic beam with an annular cross section and employing a combination of strain gauges and proximity probes to determine the dynamic shape of the tube.

The proximity probes are small devices (diameter: 5 mm, length: 35 mm) originally intended for use with rotating machinery. They provide a voltage output that is proportional to the distance between the transducer and a metallic surface. In processing the output signal, it is assumed that during the firing sequence the cannon will undergo transverse motion in both the vertical y and horizontal z directions, recoil along the central axis x, and radially expand or contract. It is also presumed that the gun tube cross section will remain circular, although the outer surface can be tapered. A minimum of three transducers are required to completely determine the translation and radial expansion of the gun at any position along its length. However, to simplify the data analysis, four transducers spaced 90 deg apart around the circumference of the tube were utilized. In this configuration, the difference in the change of the gap between transducer and gun measured by two opposing probes will yield the tube translation along

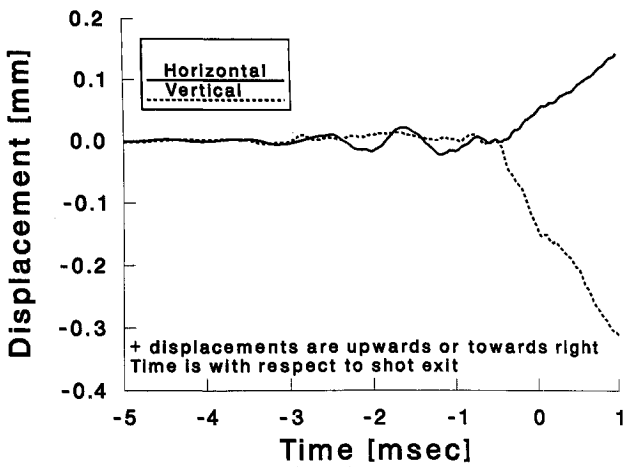

Fig. 3 Transverse motion of the gun tube near the muzzle (TPCSDS projectile).

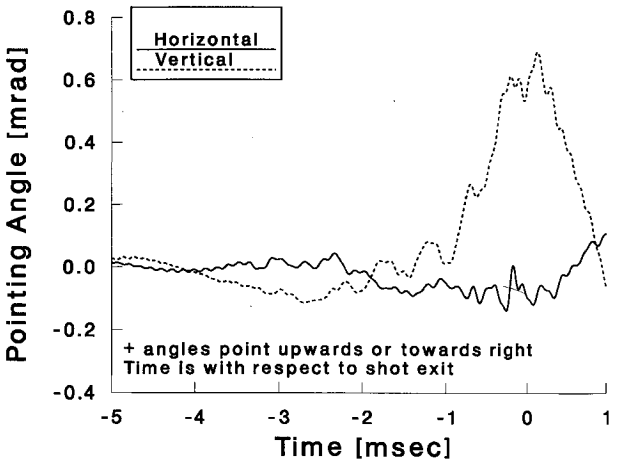

Fig. 4 Muzzle pointing angle measured by proximity probes.

the axis joining the probes. The sum of the change, when corrected for the effect of tube taper and gun motion perpendicular to the probe axis, yields the radial expansion of the tube. A complete discussion of the application of proximity probes for gun dynamics measurements can be found in Bornstein and Haug.[7]

Probes were placed at four locations along the tube: at two points in the vicinity of the muzzle (permitting the estimation of the muzzle pointing angle), near the center of the tube, and just forward of the turret. To accommodate strain gauges also mounted on the tube, the probes were placed along perpendicular axes oriented at 45 deg to the vertical and horizontal directions. Data were acquired using transient recorders possessing a pretrigger sampling capability. The instrumentation trigger signal was provided by a static pressure probe placed in close proximity to the muzzle (approximately 1 cm to the rear) that started the sampling process when the main blast wave associated with the high-pressure propellant gases reached it.

Figure 3 presents the translation of the tube measured by the four proximity probes situated near the muzzle while firing a saboted training round. A number of features are apparent in the figure; notably, the lack of any significant motion of the muzzle prior to 3 ms before shot exit, a spiral-like movement of the tube during the following 2.5 ms, and finally a rapid motion of the tube both downwards and towards the right during the final few hundred microseconds before the projectile exits the gun.

The relative tube motion at the two locations close to the muzzle permit an estimate of the muzzle pointing angle (Fig. 4). Inherent in this estimate is the assumption that the curvature of the tube between the measurement point and the muzzle is negligibly small; a criterion that cannot always be met. For these tests, the curvature in the vicinity of the muzzle was small and the proximity probes yield a good estimate of the pointing angle.

To define the dynamic tube shape, strain gauges were mounted at eight axial stations along the gun. Each station consisted of four orthogonal gauges (two each in the vertical and horizontal planes) oriented lengthwise along the tube. Diametrically opposed gauges were wired in a difference mode in the bridge completion circuits to reduce common mode signals such as hoop or pure axial stresses and to maximize the sensitivity to longitudinal bending strain. Data were initially multiplexed and recorded on analog tape that was later played back and digitized for processing by computer.

The analysis, developed by Heaps,[8] treats the gun tube as a cylindric elastic beam that can only deflect due to longitudinal bending or rigid body motion. The longitudinal bending strain is related to the local curvature of the tube. For the small values of strain encountered here, this may be accurately approximated by the second derivative of the transverse tube displacement. Performing a double spatial integration of the

strain distribution yields the displacement due to the bending or the instantaneous shape of the tube. The two constants of integration are evaluated using the tube displacements measured with proximity probes mounted near the muzzle and rear of the gun tube.

Sampling theory requires that the interval between successive data points be no larger than half of the shortest wavelength of the signal (i.e., mode shape) to be measured. If shorter wavelengths (or higher modes) are present, aliasing will occur. In the current set of measurements, bending strain was determined at nine points on the tube (eight measurements and a zero-strain condition at the muzzle), implying that the shape of the tube may be represented through a linear combination of the first four vibration modes. Based on this argument, an antialiasing, low-pass filter with a cutoff frequency of 400 Hz was employed. Once the strain data were filtered, the data at any instant of time were approximated by a polynomial function and numerically integrated.

Figures 5 and 6 depict the analysis results, presenting both the vertical and horizontal gun tube shapes during the final 2.5 ms of the projectile in-bore period, at 500-μs intervals. The in-bore trajectory of the projectile due to the vibration is also indicated. Solid circles denote the location of the projectile at instants for which the tube shape is shown. Although the propellant charge is ignited approximately 7 ms prior to shot exit, little vibration of the gun tube is observed prior to 2.5 ms before the projectile exits the muzzle.

In the vertical plane, a well-defined vibrational motion, excited by the rigid-body rotation of the gun tube about the trunnions, is observed. Two nodes are visible, one approximately two-thirds the external tube length from the muzzle and the other a short distance behind the muzzle. In the horizontal plane, the gun is constrained by the recoil system and the tube motion is more limited. The driving force for this motion is presumably interaction between the projectile and gun tube.

The muzzle pointing angle is obtained by numerically differentiating the tube displacement in the vicinity of the muzzle. The muzzle crossing velocity is obtained by determining the rate of change of muzzle displacement at shot exit.

IV. Transitional Ballistics

Projectile motion in the transitional ballistic regime, covering the region from the weapon muzzle through initial entry into undisturbed free flight, is recorded by flash radiography. A schematic representation of the x-ray setup is given in Fig. 2. Six orthogonal x-ray units are positioned in two groups of three each. The first group is placed in close proximity to the muzzle and captures the initial projectile position and orientation with respect to the line of fire. The second group is positioned further downrange, after the sabot separation process has occurred, and determines the linear and yawing motion as it enters free flight.

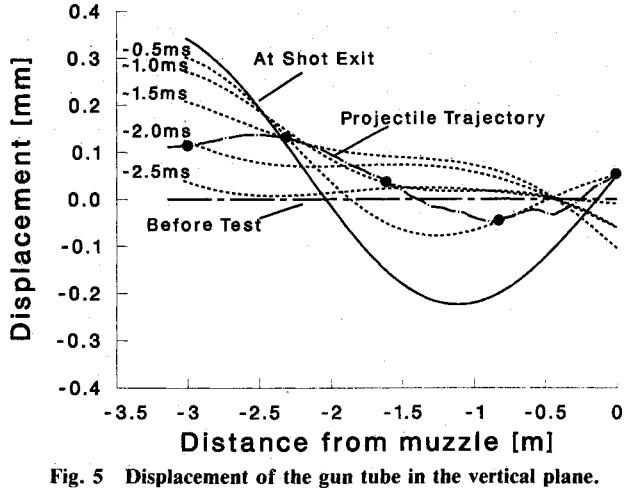

Fig. 5 Displacement of the gun tube in the vertical plane.

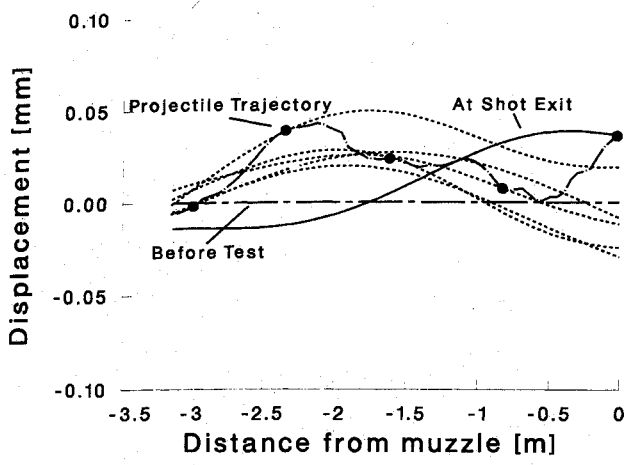

Fig. 6 Displacement of the gun tube in the horizontal plane.

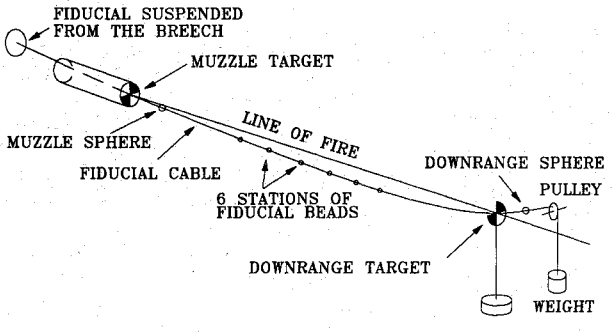

Fig. 7 Schematic representation of x-ray setup.

Six orthogonal Hewlett Packard 150-kV flash x-ray units are utilized to determine the transitional ballistics. Plywood cassettes protect the Kodak XAR840 X-Omat x-ray film which is exposed by Dupont Cronex intensifying screens bonded to the inner cassette surfaces. Both cassettes and x-ray heads are placed at a distance of approximately 1.5 m from the line of fire. This provides sufficient source-to-object distance for a single head to completely illuminate the projectile and enough object-to-cassette distance to prevent reflected shock waves from disturbing the cassette before the x ray of the projectile flight is recorded.[9] During the test, the x rays are fired sequentially, with the delay time between successive stations determined by the station separation and the projectile muzzle velocity. The initial trigger signal for the system is provided by the muzzle pressure probe used for the gun dynamics measurements.

The calibration procedure for the radiographs[10] uses a double-exposure technique. Just prior to the test, a fiducial cable is strung through the x-ray field close to the projected line of flight (Fig. 7). The x rays are pulsed at a low power level, the cable removed, and then the shot fired. The second, high-power x-ray pulse occurring as the round is launched places the image of the projectile and cable on the same radiograph.

To insure that the fiducial cable lies along the line of fire, a sighting target is placed at the far end of the x-ray array, roughly 13 m from the muzzle. A muzzle boresight is used to align this target to the sight line. The boresight is removed and a second target is placed in the muzzle of the gun, essentially locating the bore centerline. The fiducial cable is strung between these two targets taking care that the cable does not touch the targets and distort their orientation. The cable contains both fiducial beads and two sightline spheres located near the target centers. The positions of these reference markers are located in the Transonic Range coordinate system using standard surveying techniques.

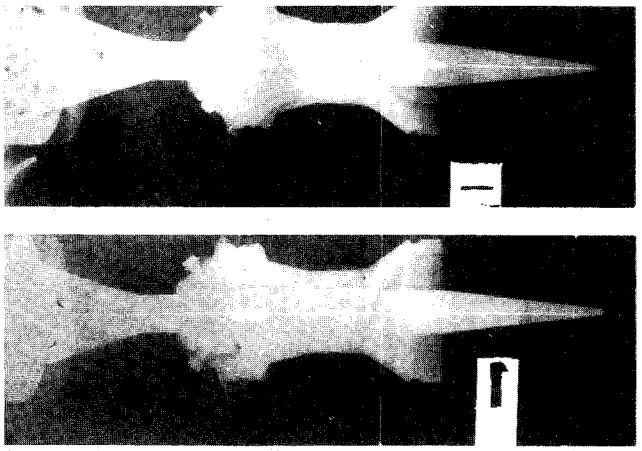

Fig. 8 Image of TPCSDS-T projectile at launch.

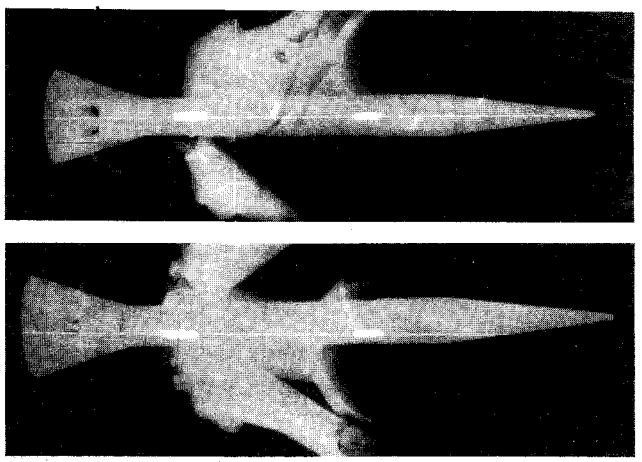

Fig. 9 Image of TPCSDS-T projectile approximately 3 m downrange of the muzzle.

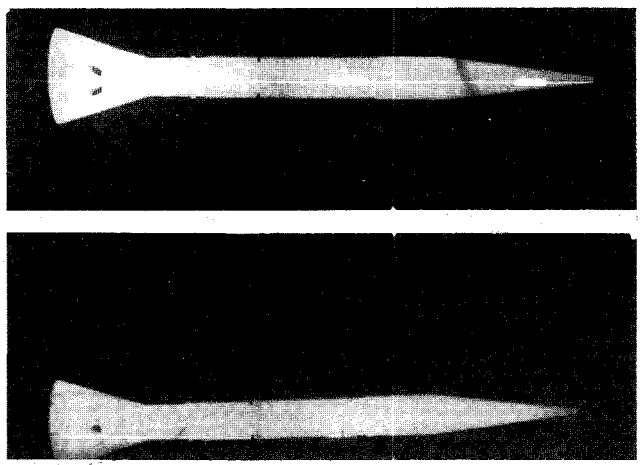

Fig. 10 Image of TPCSDS-T projectile entering free flight.

Figure 8 is a set of orthogonal views of a cone-stabilized, discarding sabot training projectile (TPCSDS) as it is launched from the gun tube. The upper portion of the photograph is a view of the projectile taken from below, whereas the lower image is a side view of the projectile. Immediately after disengagement from the gun tube, the sabot components remain essentially in the as-fired position. In this example, the cone base of the projectile is just clearing the muzzle. The recoiling motion of the muzzle can also be observed, with the fainter image of the muzzle corresponding to its position prior to the test and the more intense image corresponding to the muzzle as the projectile exits the gun.

Also visible in the photograph are the fiducial cable and the two reference beads for this station. As part of the calibration procedure, the distance between the notches in each of the beads is measured. Comparison of this distance with the corresponding distance between these two points in the x-ray image yields an in-situ determination of the magnification factor for each x ray, eliminating the necessity to accurately measure the distance between each head and the object and film planes.

Just downrange of the muzzle, the components begin to rotate off the flight body. Contact is maintained between the aft end of the sabot and the projectile until the third x-ray station (Fig. 9). In the figure, one of the sabot petals has already lifted off at the rear, an excellent example of a discard asymmetry. In the side view, one can also see a significant pitch angle between the projectile and the fiducial cable developing.

Between the third and fourth stations, the components lift away and only aerodynamic interaction continues. By the time the projectile reaches the second set of three x-ray stations, the sabot components are still within the x-ray field of view, but have moved sufficiently far from the flight body to preclude further interaction and the projectile is in undisturbed free flight (Fig. 10).

The motion of the c.g. of a saboted projectile through the x-ray system is presented in Figs. 11 and 12, together with the measured line of fire. In the figures, the x axis corresponds to the downrange coordinate, whereas the y and z axes correspond to the vertical and horizontal coordinates, respectively.

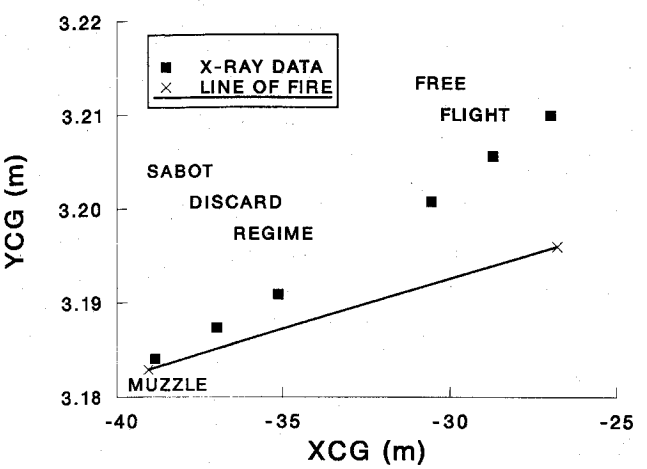

Fig. 11 Center-of-gravity trajectory of TPCSDS-T projectile in the vertical plane.

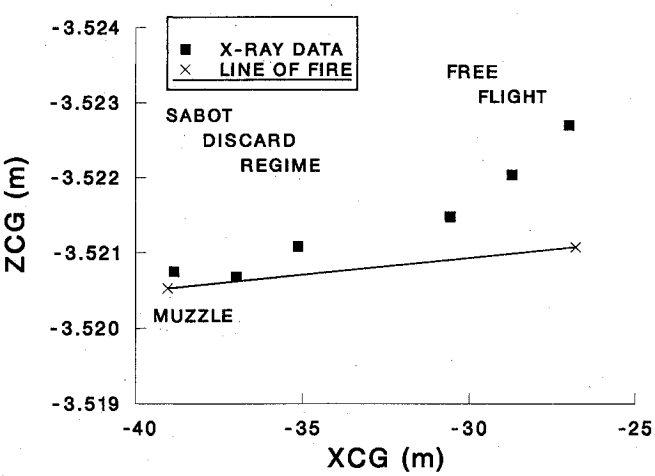

Fig. 12 Center-of-gravity trajectory of TPCSDS-T projectile in the horizontal plane.

The plot of the projectile vertical motion shows that the projectile begins its trajectory at a point in space near the static muzzle location but with a "separation angle" above the line of fire. This angle is the component of the total jump representing the sum of all perturbations seen by the projectile up to this point, including gun tube, mechanical discard, muzzle blast, and initial sabot discard disturbances. During passage of the projectile through the first three x-ray stations, the projectile does not appear to be subjected to any significant accelerations and its trajectory can be approximated by a straight line.

In the horizontal plane (Fig. 12), the projectile is to the right of the line of fire; the trajectory again is at a small angle with respect to the line of fire. Because of the smaller deflection in the horizontal plane, errors in the determination of the projectile center of gravity location from the x rays are more apparent in this plot. The scale of these errors is of the same order as the 0.5-mm accuracy to which the original x rays can be read. The c.g. trajectory is still approximated by a linear fit.

Between the first and second x-ray groups, the sabot discard process goes to completion. Further alterations to the trajectory, leading to an initial free-flight departure angle, may occur in this region. The differences in the muzzle separation and initial free flight departure angles are more apparent in the horizontal plane in this example, though this is by no means the rule.

To this point, the x-ray data have been utilized to consider only the linear motion of the projectile. However, the contributions of launch dynamics to total jump are not completely defined until the aerodynamic jump (or jump due to yaw) has been treated. The angular motion of the projectile as a function of the downrange location is shown in Figs. 13 and 14.

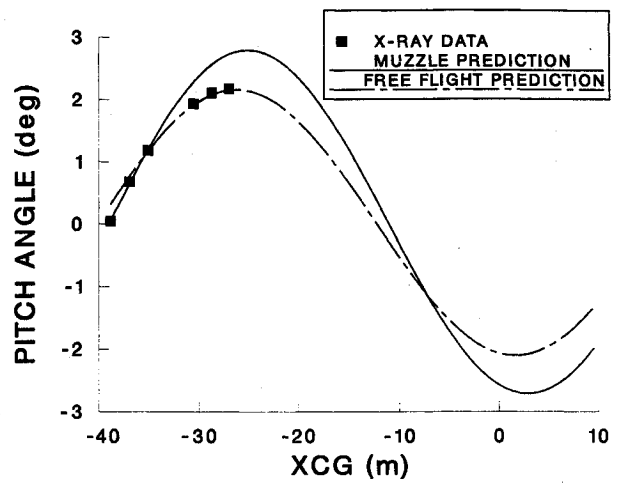

Fig. 13 Pitch history for TPCSDS-T projectile determined from x-ray data.

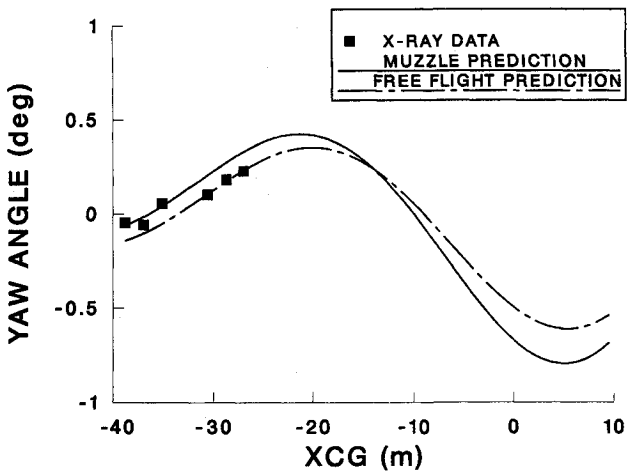

Fig. 14 Yaw history for TPCSDS-T projectile determined from x-ray data.

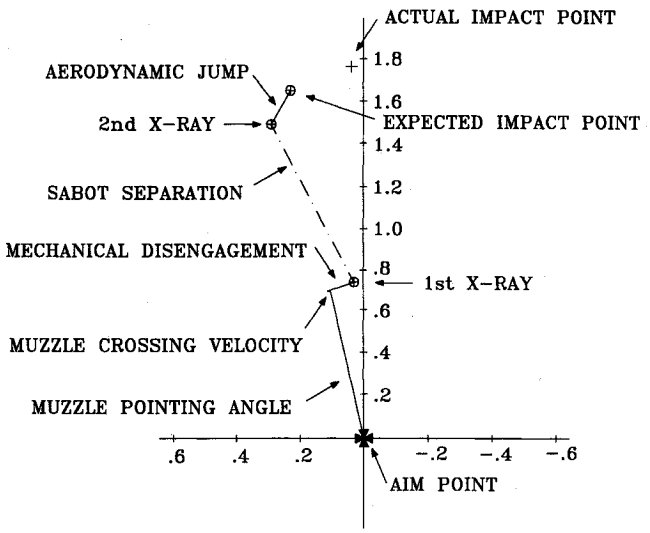

Fig. 15 Closure diagram for TPCSDS-T projectile.

The data indicate that the projectile is launched with very small yaw, consistent with the strong constraints provided by the sabot components and the gun tube. The round has a finite angular velocity about its center of gravity (or yaw rate) as it exits the cannon and the yaw angle grows accordingly. This is more apparent in the vertical plane, where the yaw angle has grown to approximately 1.25 deg at the third x-ray station, than in the horizontal plane, where the yaw measured at the first three stations is less than 0.1 deg or roughly the order of the estimated accuracy (± 0.1 deg) that can be obtained from a good quality x ray. In the figure, the squares represent the yaw angles determined from the x rays, whereas the solid line is a prediction of the yawing motion of the projectile based on the measured angular rate in the first three x-ray stations (i.e., prior to sabot separation) and a knowledge of the aerodynamic coefficients for the projectile.

As the round moves through the sabot discard region, it is subjected to angular disturbances caused by asymmetries in the discard process that modify the yawing motion. The dashed curve represents the predicted free-flight yaw behavior based on the angular rate measured in x-ray stations 4–6. These yaw rates can be used to compute the projectile free-flight aerodynamic jump.[3]

V. Closure Analysis

Figure 15 depicts the closure analysis, introduced in Sec. II. The muzzle pointing angle makes a significant contribution to the overall jump, providing a disturbance of approximately 0.45 mils. The crossing velocity contribution is significantly smaller, roughly 0.12 mils. Experience gained firing a number of these rounds has shown that the round-to-round variation for both the magnitude and orientation of these vectors will be small.

The trajectory of the projectile just after it has been launched, but before sabot discard has occurred, is represented by the point marked first x ray. The effects of in-bore projectile motion, muzzle blast, and tip-off disturbances have been lumped together into the vector that joins this point and the tip of the muzzle crossing velocity vector. The magnitude of this vector is comparable to the muzzle pointing angle. However, the observed variation of both the magnitude and orientation was larger than observed for the gun dynamics vectors. This was also found to be the case for the sabot discard disturbance, represented by the vector joining the trajectories determined from the first and second groups of x rays. Lastly, for this

round the magnitude of the yawing motion was small therefore the aerodynamic jump was also small. The tip of the vector representing aerodynamic jump is the angular coordinate for the expected impact point of the projectile, once the effect of gravity drop has been removed. As the figure indicates, the difference between this point and the actual impact is approximately 0.17 mils, within the 0.2-mil accuracy we attribute to the measurement techniques.

VI. Concluding Remarks

This paper has briefly discussed the methodology and measurement techniques which have been developed at BRL to quantitatively determine the contribution of individual disturbance sources to the overall jump of a projectile. The technique has been applied with success to both saboted and full-bore ammunition for the 105-mm M68A1 and 120-mm M256 Cannon used by the M1 and M1A1 tanks. Similar methods, on a smaller scale, are also currently being used to examine the performance of 25-mm ammunition.

References

[1]Gay, H. P., and Elder, A. S., "The Lateral Motion of a Tank Gun and Its Effect on the Accuracy of Fire," U.S. Army Ballistic Research Lab., BRL Rept. 1070, Aberdeen Proving Ground, MD, March 1959.

[2]Plostins, P., "Launch Dynamics of APFSDS Ammunition," U.S. Army Ballistic Research Lab., BRL TR-2595, Aberdeen Proving Ground, MD, Oct. 1984.

[3]Murphy, C. H., "Free Flight Motion of Symmetric Missiles," U.S. Army Ballistic Research Lab., BRL Rept. 1216, Aberdeen Proving Ground, MD, July 1963.

[4]Biele, J. K., "The Relationship of Gun Dynamics to Accuracy in a 120 mm Tank Gun," *Proceedings of the 8th International Symposium on Ballistics,* American Defense Preparedness Association, Arlington, VA, Oct. 1984, pp. LD11–LD16.

[5]Schmidt, J. Q., and Andrews, T. D., " Description of the Joint BRL-RARDE 40 mm Experiment to Assess Projectile Launch Parameter Measurement Techniques," U.S. Army Ballistic Research Lab., BRL TR-2679, Aberdeen Proving Ground, MD, Sept. 1985.

[6]Simkins, T. E., Scanlon, R. D., and Benedict, R., "Transverse Motion of an Elastic Supported 30 mm Gun Tube During Firing," *Proceedings of the Third U.S. Army Symposium on Gun Dynamics,* Benet Weapons Lab., Watervliet, NY, May 1982, pp. I71–I92.

[7]Bornstein, J. A., and Haug, B. T., "Gun Dynamics Measurements for Tank Gun Systems," U.S. Army Ballistic Research Lab., BRL MR-3688, Aberdeen Proving Ground, MD, April 1988.

[8]Heaps, C. W., "Determination of Gun Tube Motion from Strain Measurements," U.S. Army Ballistic Research Lab., BRL-MR-3562, Aberdeen Proving Ground, MD, March 1987.

[9]Schmidt, E. M., Plostins, P., and Bundy, M. L., "Flash Radiographic Diagnostics of Projectile Launch," *Proceedings of 1984 Flash Radiography Symposium*, American Society for Nondestructive Testing, Columbus, OH, May 1984, pp. 100–108.

[10]Schmidt, E. M., and Shear, D. D., "Aerodynamic Interference During Sabot Discard," U.S. Army Ballistic Research Lab., BRL Rept. R-2019, Aberdeen Proving Ground, MD, Sept. 1977.

James E. Daywitt
Associate Editor